



# A comparative analysis of the puncturing abilities of cephalopod beak rostra using engineering tools

Simeng Wang<sup>1</sup> · Marius Didziokas<sup>1</sup> · Marjorie Roscian<sup>2</sup> · Susan Evans<sup>3</sup> · Isabelle Rouget<sup>4</sup> · Anthony Herrel<sup>5,6,7,8</sup> · Mehran Moazen<sup>1</sup> · Louise Souquet<sup>1</sup>

Received: 6 February 2024 / Accepted: 28 April 2024  
© The Author(s) 2024

## Abstract

Cephalopods, a diverse class of carnivorous marine predators, exhibit a wide range of feeding behaviours and foraging strategies related to their lifestyle, habitat and morphological adaptations. Their beaks play a crucial role in capturing and processing prey. This study investigates the link between the shape of the rostrum of cephalopod beaks and their function through a mix of experimental and computational approaches. Fourteen upper beak rostrum models from a range of cephalopod species, representing their morphological and ecological diversity, were 3D-printed, and subjected to uniaxial puncture tests. Force and displacement were recorded to estimate puncture ability. Finite Element Analysis (FEA) was used to explore the form–function relationship under loading conditions mimicking biting and pulling, analysing stress patterns across different rostrum morphologies. The results show that rostrum size significantly influenced puncture performance, with smaller rostra requiring less force and displacement for puncturing. However, larger rostra exhibited higher structural stiffness, suggesting increased vulnerability to stress during biting. Morphology-driven tests demonstrated species-specific differences in puncture abilities, with rostrum sharpness playing a crucial role. FEA results further indicated that longer and sharper rostra were more susceptible to stress, potentially impacting their overall structural integrity. The findings highlight the trade-off between rostrum size and sharpness in cephalopod beaks, with implications for prey selection and feeding efficiency. The study contributes to understanding the morpho-functional aspects of cephalopod beaks and their role in prey capture and consumption, shedding light on the evolutionary pressures shaping these remarkable marine predators.

**Keywords** Beaks · Morphology · Cuttlefish · Squid · Octopod · Diet · 3D modelling

## Introduction

Cephalopods are a cosmopolitan and diverse class of carnivorous marine predators. This group is divided in two sub classes, the outer-shelled nautiloids and the inner-shelled coleoids. The later represent the large majority of the group, including squids, cuttlefishes, and octopuses. In total, approximately 800 species have been described living in all seas and oceans around the world, from the surface to the abyss (Jereb et al. 2014; Jereb and Roper 2005, 2010). This diversity in taxonomy, morphology and habitat use is reflected in their diet (Rodhouse and Nigmatullin 1996; Cherrel and Hobson 2005; Villanueva et al. 2017). A variety of feeding behaviours is observed in cephalopods, and

species feed on a wide variety of prey (e.g., crustaceans, molluscs, bivalves, teleost fish or even other cephalopods). Differences in diet between species have been described depending on their habitat, with benthic species incorporating a larger proportion of crustaceans, while pelagic species incorporate more fish into their diet (Nixon 1987; Sup. Table 1). Although coastal species have attracted more attention due to their accessibility and economic importance in fisheries, the majority of cephalopod species are difficult to access and details of their diet remain unknown (Villanueva et al. 2017; Ibanez et al. 2021).

The cephalopod feeding apparatus is composed of two beaks and a radula embedded in a mass of masticatory muscles (Bidder et al. 1966; Kear 1994; Messenger and Young 1999; Uyeno and Kier 2005; Roscian et al. 2023). Together, they form the buccal mass located in the centre of the arm crown (Fig. 1). While the arms are used to capture, manipulate, and maintain the prey, the beak is the principal structure

---

Responsible Editor: A.G. Checa.

Extended author information available on the last page of the article

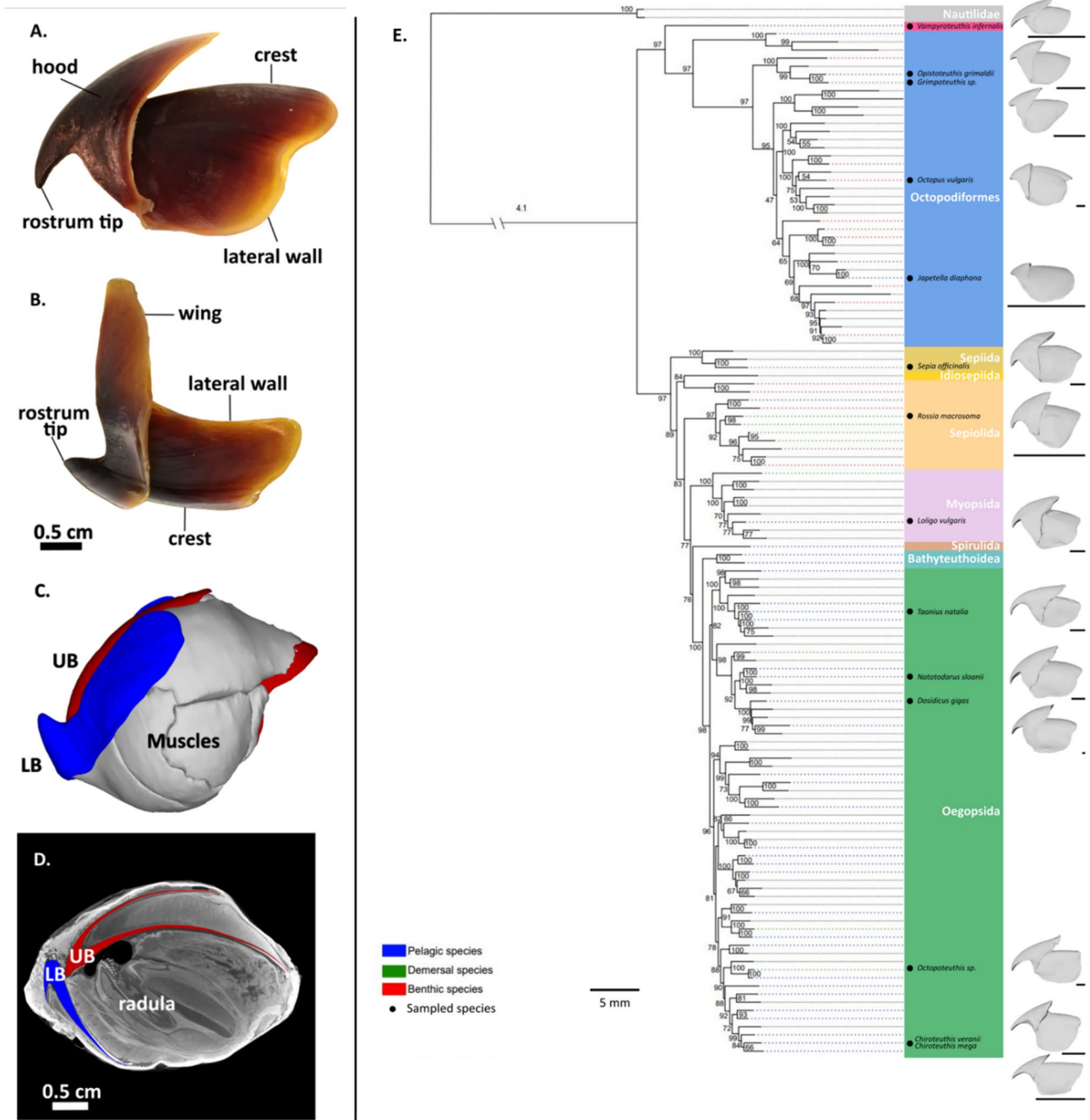


**Fig. 1** Cephalopod beak anatomy and diversity. *Sepia officinalis* **A.** upper beak (UB, red) and **B.** lower beak (LB, blue) in lateral view, **C.** buccal mass 3D model and **D.** CT scan sagittal section. **E.** Cepha-

lopod phylogeny with upper beaks of species included in this study. **A–D.** are adapted from Roscian et al. 2023. **E.** is adapted from Roscian et al. 2022

responsible for biting and the break-down of prey into bite-sized pieces (Bider et al. 1966; Altman and Nixon 1970; Uyeno and Kier 2007). Unlike in vertebrates, the cephalopod upper beak is nested within the lower one, the anterior-most aboral face of the upper beak being in contact with the oral face of the lower one when the beak is fully closed (Fig. 1). Beaks display an important variability in shape, the lower

beak being extensively used for taxonomy (Clarke 1962, 1986; Xavier and Cherrel 2021). A recent study, however, showed that the beak morphology, and especially that of the upper beak, does not only reflect the phylogeny of the group but also their habitat and trophic level, suggesting that beak morphology may reflect adaptation to diet (Roscian et al. 2022). Therefore, cephalopods beaks may be used in

a morpho-functional framework to explore feeding abilities and potential adaptations to diet.

As the large majority of cephalopod species are not accessible for in vivo observations and measurements, exploring feeding performances and potential adaptations across cephalopods requires the use of experimentation on proxies and computational models. Engineering techniques enable us to isolate and test different factors potentially affecting puncture efficiency, such as rostral size and shape. The rostrum is the part of the beak interacting with the prey during a bite. The rostrum is responsible for the initial puncture, while the edges probably act later in a shearing motion (Souquet et al. 2023). The rostrum puncture ability is considered herein, because the functional abilities of the rostrum to initially puncture a prey item will determine the range of potential diet.

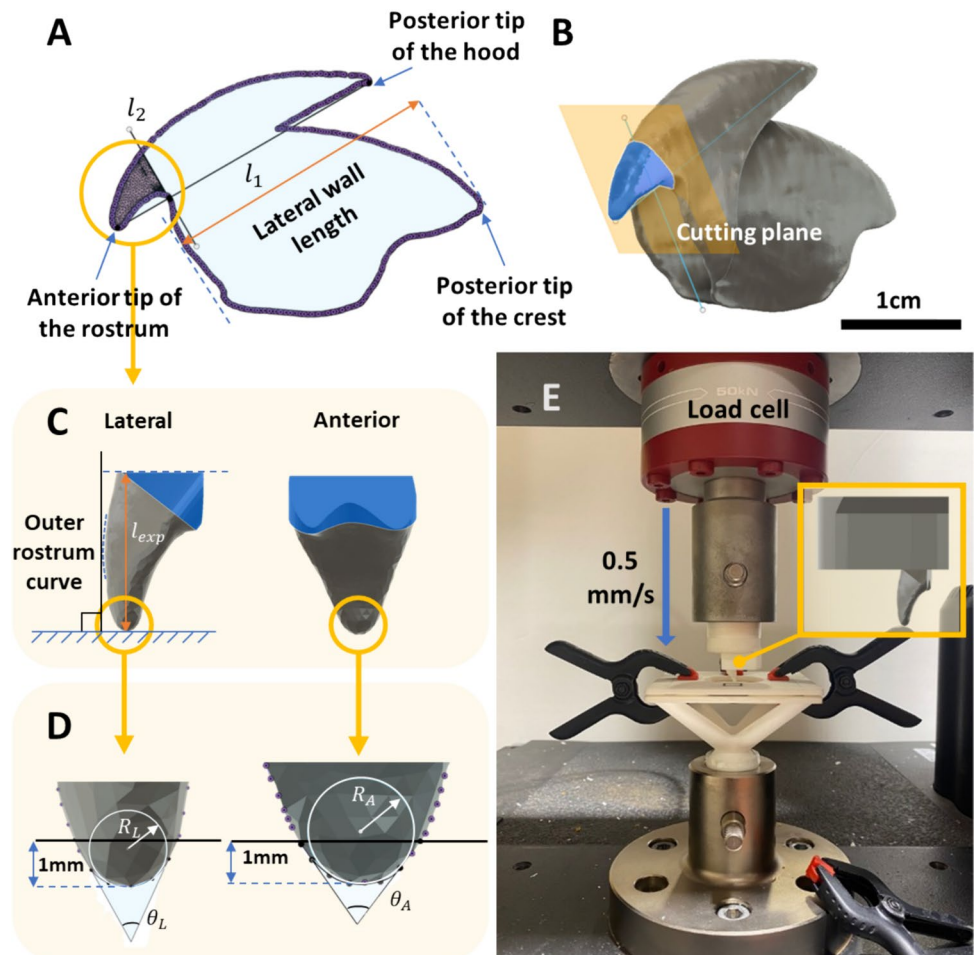
The overall aim of this study was to investigate the link between the shape of the rostrum of cephalopod beaks and their puncture efficiency. Specifically, we aimed to (1) experimentally mimic biting in a sample representing the morphological and ecological diversity of cephalopods to investigate how rostrum morphology affects puncture

efficiency; and (2) computationally study how different rostrum morphologies tolerate mechanical stress during biting to provide insights into the potential trade-off between puncture efficiency and structural integrity.

### Materials and methods

Fourteen upper beaks were selected from a pre-existing 3D dataset (Roscian et al. 2022), chosen to span the range of morphological beak variation, with a special focus on rostrum shape, as well as representing all major families, and a range of different habitats (benthic, demersal, and pelagic; Fig. 1). First, a series of uniaxial puncture tests was performed on a target material using 3D-printed upper beak rostra (Fig. 2). Force and displacement data were recorded and used as indicators of puncture efficiency. Secondly, Finite Element Analysis (FEA) was performed to explore the form–function relationships under loading conditions mimicking biting and pulling to quantify the stress pattern across the rostrum morphologies considered.

**Fig. 2** Illustration of the cephalopod upper beak rostrum preparation method and puncture test setup. **A** Lateral view of the projected *Sepia officinalis* upper beak 3D model with the planes used for rostrum isolation and the measurement of lateral wall length. **B** Rendered view of the *Sepia officinalis* upper beak 3D model showing the isolation plane (yellow) and the isolated rostrum (blue). **C** Lateral and anterior views of the *Sepia officinalis* isolated rostrum and the supporting material (in blue) for the morphology-driven puncture test. The rostrum was rotated to an orientation perpendicular to the horizontal plane ( $l_{exp}$ : Length of the experimentally tested rostra;  $A_{exp}$ : Base area of the experimentally tested rostra). **D** Illustration of the rostrum tip lateral included angle  $\theta_L$ , anterior included angle  $\theta_A$  and sharpness index measurements. **E** Full puncture test setup on the Instron machine. The tip of the rostrum, the centre of the mounting platform and the centre of the target sheet fixture are on the same centred vertical line



## Beak sampling

The upper beak models for this test were selected based on a variety of morphologies (Fig. 1) covering the major cephalopod families including: eight-armed decapods: pelagic squids (Oegopsida, 6), coastal squids (Myopsida, 1), cuttlefishes (Sepiida, 1) and Bobtail squid (Sepiolida, 1); ten-armed octopods: octopuses (Octopodiformes, 4) and vampire squid (Vampyromorpha, 1). The 3D model of a *Sepia officinalis* adult beak (Fig. 1A–D) used in the size-driven puncture tests was based on Souquet et al. (2023). The cephalopod beak models of all other 13 species (Fig. 1) used for the morphology-driven puncture test were obtained from Roscian et al. (2022). For all species, the upper beak rostra were isolated in Fusion 360 (Autodesk, CA, USA—Fig. 2A, B). To do this, a straight line ( $l_1$ ) was first drawn connecting the anterior tip of the rostrum and the posterior tip of the hood (Fig. 2A). A second line  $l_2$  perpendicular to  $l_1$  was created to go through the highest point of curvature of the jaw angle (Fig. 2A). A construction plane was created along  $l_2$  and perpendicular to  $l_1$  to digitally isolate the rostrum in a reproducible way (Fig. 2B).

## 3D printing

In order to create a 3D printed physical model that could be attached to the puncture testing machine, a mounting platform was designed, and all the isolated rostra were aligned and positioned so that the anterior tip of the rostrum was centred and tangent to the target material (Fig. 2E). The dorsal extremity of the rostrum was placed on the support platform, and the rostrum cutting plane was extruded perpendicularly to the platform for attachment (Fig. 2E). The platform and rostrum were merged to be printed as a single object. A target mounting base was designed using Fusion 360 to hold a thin rectangular piece of target material to puncture (Sup. Figure 1). To isolate the effect of size alone, a 3D model of a *Sepia officinalis* rostrum was scaled up uniformly in all directions by a factor from 1 to 4 with an interval of 0.5 between each replicate using Fusion 360. To test the effect of rostrum shape as observed across different species, 3D models of the entire beak of all 13 species were scaled up to the same lateral wall length, measured in lateral view as the distance from the posterior end of the crest to the highest point of curvature of the jaw angle (Fig. 2A). This minimises the effect of beak size, without masking the effect of rostrum length which is an important part of rostral shape variability. As the machine used in this study requires a minimum rostrum size of 5mm to ensure the feasibility of the test, all rostra, after the initial scaling, were scaled up uniformly with the same factor so that the smallest rostrum was 5mm long. In addition, an attachment piece was designed in Fusion 360 to fix the rostrum platform

to the machine, as well as a target holder (Fig. 2E, Sup. Figure 1). All 3D models including the rostra attached to their platforms, the platform attachment piece and the target holder were 3D printed, using the Selective Laser Sintering (SLS) technique on the EOS Formiga P100 machine, PA 2200 filament (nylon powder, Young's modulus = 1.7 GPa, EOS GmbH, 2008) and smooth surface finishing.

## Target material

The target material was selected to be homogeneous and resistant, yet brittle enough to produce a puncture force during the experiment. This target simulates a prey item with linear elastic behaviour. We chose 0.13mm thick dry agar sheets composed of 90% gelling agent agar (E406) and 10% stabiliser glycerol (E422) produced by Inka foods company (CA, USA). Young's modulus of the target sheet was  $1.33 \pm 0.14$  GPa, measured using a standardized uniaxial tensile test (for details, see Sup. Material).

## Puncture test

Two series of uniaxial puncture tests were conducted to investigate the effect of rostrum size and morphology on puncture ability (Fig. 3A). Both series of tests were conducted on an Instron 5944 single-column tensile tester with a 50kN load cell (INSTRON, MA, USA—Fig. 2E) under displacement-controlled compression. The dry agar sheets were cut into squares and placed into the target holder, and the rostrum platform was fixed to the attachment piece (Fig. 2E). Once these elements are connected to the testing machine, the rostrum was moved as close as possible to the target without creating any reaction force, i.e., without touching the sheet, setting the reference position to measure displacement. For size-driven tests, each rostrum was used to puncture five different sheets ( $n=5$  replicates per size). For morphology-driven tests, each rostrum was used to puncture two different sheets ( $n=2$  replicates per species). The force (N) and the displacement (mm) were recorded, the averaged penetration forces, the averaged penetration displacements, and the averaged slope of the linear regime of the force–displacement graph (i.e., effective stiffness estimates; van de Berg et al. 2017) were calculated.

## FEA models

Finite Element Analysis (FEA) were conducted using ANSYS workbench (ANSYS Inc., PA, USA). The set of isolated rostrum 3D models used for 3D printing was oriented so that the rostrum tip angle bisector in lateral and frontal view was perpendicular to a horizontal target plane (Fig. 2). Each was meshed with ca. 85,000 10-node tetrahedral elements (following a mesh convergence study to find the minimum

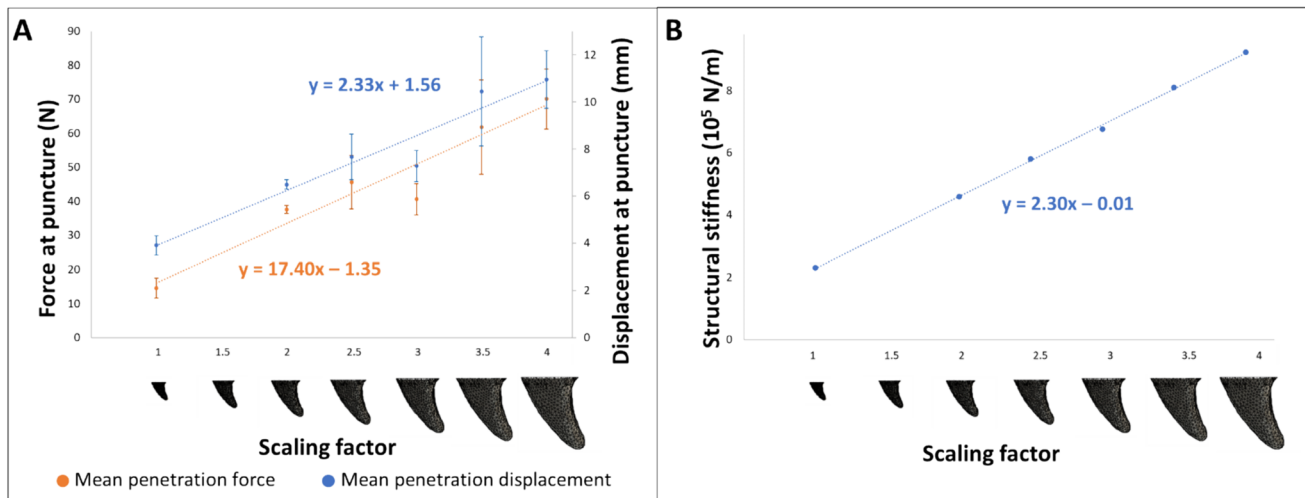


**Fig. 3** Linear regression of the variable obtained from puncture tests and FEA against scaling factor for *Sepia officinalis* rostra. **A** Maximum puncture force and maximum puncture displacement against size (uniform scaling factor) of the *Sepia officinalis* upper beak rostra

**B** Structural stiffness (obtained from the FEA compression test) against size (uniform scaling factor) of the *Sepia officinalis* upper beak rostra

number of elements to be used without loss of accuracy). Rostra were modelled as an isotropic elastic material with a Young's modulus of 1.7GPa (same as the PA 2200 material) and an estimated Poisson's ratio of 0.33. Compression tests on the *Sepia officinalis* rostra with different sizes and the 14 selected species were simulated. The rostrum base was constrained in all directions, and a 20N load was applied against the rostrum along the axial direction on the tip area (roughly 1/12 of the rostrum length; Figs. 5A; 6A). The rostrum structural stiffness, which is characterised by the material and shape of the rostrum, and illustrates the rostrum resistance to deformation and the load-carrying ability, was also calculated from this test as:

$$k = \frac{20N}{\text{maximum deflection along the load direction}}$$

Next, a dragging simulation was conducted on the same rostrum samples (size and shape datasets) to mimic the upper beak retraction during the bite cycle (Kear 1994; Uyeno and Kier 2005, 2007). The rostrum base was constrained in all directions, and the 20N force was applied on half of the rostrum inner face (Figs. 4B, 6B). The von Mises stress pattern is shown for each test in the anterior, lateral, and dorsal view.

### Morphological and Statistical analysis

The rostra were all characterised by: (i) the anterior and lateral rostrum tip included angles (Fig. 2D), (ii) the sharpness index (radius of curvature of the rostrum tip; Fig. 2D), (iii) length ( $l_{\text{exp}}$ ; Fig. 2C), (iv) base area, (v) total volume.

The beak rostrum anterior tip included angle ( $\theta_A$  in  $^\circ$ ) and the lateral tip included angle ( $\theta_L$  in  $^\circ$ ) were measured from 1mm above the tips (Fig. 2C, D). The sharpness index was quantified following the method described by Freeman and Weins (1997) as:

$$\text{Sharpness index} = \frac{1}{\sqrt[3]{\frac{1}{R_A} + \frac{1}{R_L}}}$$

where  $R_A$  (in mm) is the anterior radius of curvature and  $R_L$  (in mm) is the rostrum lateral radius of curvature.  $R_A$  and  $R_L$  were obtained from the fitted circles at the rostrum tips (Fig. 2D). Contrary to the included angles, sharpness index is affected by age and wear. These two metrics are therefore useful to use together to quantify rostrum tip morphology (Anderson 2018).

The length of the rostrum was measured as the vertical distances from the anterior tips of the rostra to the mounting platforms (Fig. 2C) or the top surface for FEA (Fig. 6C). The base areas for the experimental samples were obtained as the contacting areas between the rostra and the mounting platforms, and the ones for the FEA tests were the flat upper surface area. The volume was taken as the total volume of the rostrum with the supporting materials where available (but without the mounting tool).

Linear regressions were performed using the Excel Analysis ToolPak. One-way ANOVA with a significance level of p-value < 0.05 was used. The linear regression coefficient, standard error, R square, F-value and p-value were calculated.

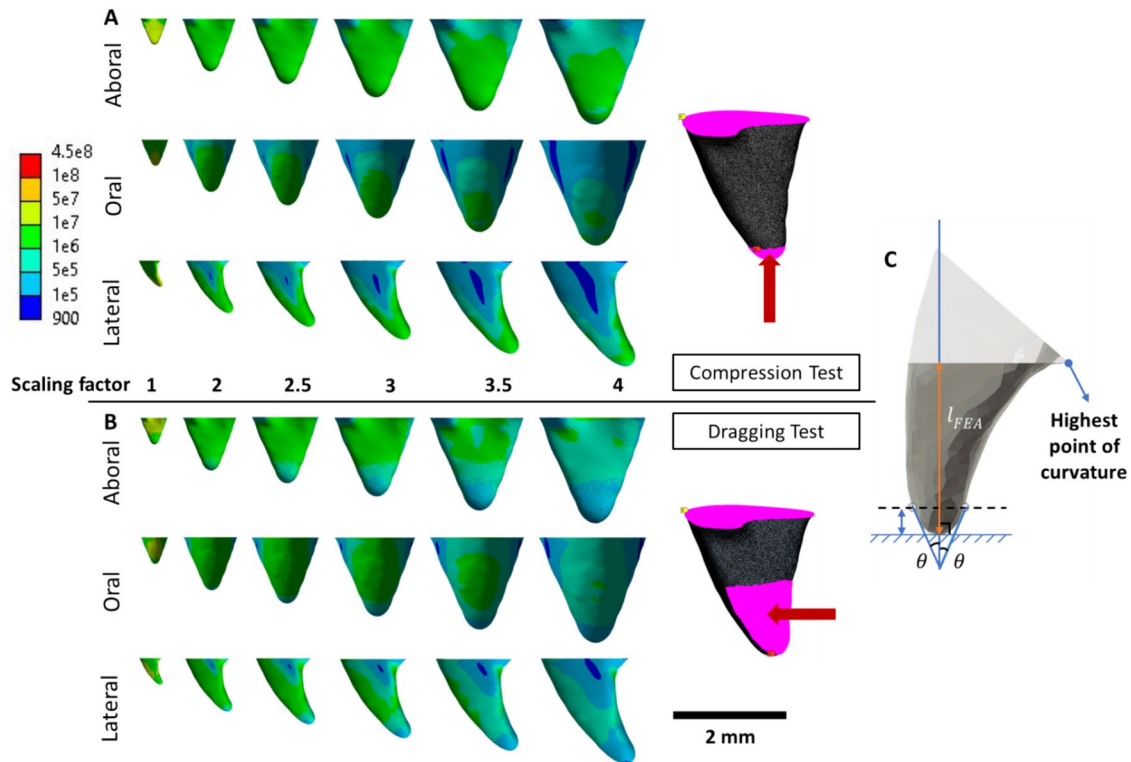


**Fig. 4** FEA compression and dragging test results on the *Sepia officinalis* rostra with different scaling factors. **A** Von Mises stress pattern plots for the compression test. **B** Von Mises stress pattern plots for the dragging test. For both, the constraints and loads are illustrated on the

rostra on the right (pink, red arrow represent the load direction). **C** Illustration of the rostrum orientation and cutting methods. Stress pattern colour legend is in Pa

## Results

### Size-driven tests

During the puncture experiment, no puncture was obtained for the 1.5 scaling factor, probably due to an operator error during the test. Therefore, no results were recorded for this rostrum size, and it was removed from the statistical analysis. The mean penetration force (N) and mean penetration displacement (mm) were both positively and linearly correlated with the scaling factor ( $R^2 = 0.95$  and  $p = 0.001$  for both; Table 1, Fig. 3A), meaning that a larger rostrum required more force and more displacement than smaller ones to puncture a given tissue. No significant correlation was found between the slope of the linear region of the force–displacement graph (i.e., effective stiffness estimates; van de Berg et al. 2017) and the rostrum size ( $R^2 = 0.47$ ,  $p = 0.131$ ; Table 1), meaning that the force required to produce one unit of displacement remains constant regardless of the size of the beak. Regarding the FEA analysis, a strong correlation was observed between the upper beak rostrum size and the rostrum's structural stiffness ( $p < 0.001$ ; Fig. 3B). The von Mises stress patterns showed that smaller rostra experienced higher stresses in response

to a given force than the larger ones (Fig. 4). This indicates that although smaller beaks have higher puncture ability (Fig. 3A), they are at a higher risk of failure.

### Morphology-driven puncture test

The 3D-printed rostra of different species of cephalopods required different forces to puncture the target sheets (Fig. 5A). *Octopus vulgaris*, *Grimpoteuthis sp.* and *Japetella diaphana* rostra did not puncture the target at the max displacement used in this experiment (6mm, corresponding to a force comprised between 30 and 35N depending on the species). These three species have short and blunt rostra with a larger anterior and lateral rostrum tip angle, and a high sharpness index. Apart from these three, the *Sepia officinalis* rostrum required the largest force to puncture the target material while the *Octopoteuthis sp.* rostrum required the lowest force (Fig. 5A). Contrary to the size-driven puncture results, here the effective stiffness estimate (slope of the linear region of the force displacement graph) showed differences between species, with the *Taonius natalia* rostrum having the lowest values indicating that a smaller force was necessary to obtain a given displacement compared to other species. In contrast, the *Japetella diaphana* rostrum

**Table 1** The statistical analysis of the size and morphology driven puncture tests (N: number of tests for each rostrum sample; Bold numbers: p-value < 0.05)

Test parameter	Beak characteristic	N	Linear regression coefficient	Standard error	R square	F	P-value (significant F)
Penetration force	Rostrum scaling factor	5	1.08	0.13	0.95	71.87	<b>0.001</b>
	Rostrum length	2	-0.32	0.33	0.10	0.96	0.353
	Rostrum base area	2	0.05	0.13	0.02	0.15	0.705
	Rostrum volume	2	-0.005	0.01	0.03	0.24	0.633
	Anterior included angle	2	0.16	0.13	0.15	1.56	0.244
	Lateral included angle	2	0.20	0.12	0.23	2.71	0.134
	Sharpness index	2	50.76	10.90	0.71	21.69	<b>0.001</b>
Penetration displacement	Rostrum scaling factor	5	0.73	0.09	0.95	73.19	<b>0.001</b>
	Rostrum length	2	-0.05	0.05	0.11	1.06	0.330
	Rostrum base area	2	0.007	0.02	0.01	0.13	0.725
	Rostrum volume	2	-0.0009	0.0014	0.04	0.41	0.539
	Anterior included angle	2	0.02	0.02	0.10	1.02	0.339
	Lateral included angle	2	0.03	0.02	0.23	2.76	0.131
	Sharpness index	2	6.48	1.72	0.61	14.21	<b>0.004</b>
Slope of the linear region	Rostrum scaling factor	5	0.18	0.09	0.47	3.60	0.131
	Rostrum length	2	-0.18	0.06	0.40	7.99	<b>0.015</b>
	Rostrum base area	2	0.03	0.03	0.06	0.74	0.407
	Rostrum volume	2	-0.004	0.003	0.14	1.87	0.196
	Anterior included angle	2	0.04	0.01	0.83	58.77	< <b>0.001</b>
	Lateral included angle	2	0.05	0.01	0.68	26.00	< <b>0.001</b>
	Sharpness index	2	10.80	2.05	0.70	27.61	< <b>0.001</b>

required the largest force to reach the displacements and failed to pierce through the target material. The penetration force (Fig. 5B,  $p=0.01$ ) and displacement (Fig. 5C,  $p=0.04$ ) were positively correlated with the rostrum sharpness index, meaning that sharp beaks (with low index values) require smaller forces and displacements to puncture a given target (Table 1). The effective stiffness estimated was positively correlated with the rostrum length, rostrum anterior and lateral tip angles, and the sharpness index (respectively,  $p=0.015$ , others < 0.001; Fig. 5D, Table 1), indicating that sharp rostra with a small tip angle require lower force to obtain a given displacement.

### FEA compression and dragging tests

The rostrum structural stiffness increased with the rostrum lateral tip angle (Fig. 5E,  $p=0.008$ ) and the beak sharpness index (Fig. 5E,  $p=0.004$ ) and decreased with the rostrum length (Fig. 5F,  $p=0.02$ ) meaning that long and sharp beaks are more prone to failure (Fig. 6; Table 2). The penetration force, displacement, and the linear region slope were also positively correlated with the rostrum structural stiffness ( $p=0.003$ , 0.01 and 0.045, respectively; Table 2). Under compression, most specimens showed higher stress on the aboral face of the rostrum, with the exception of *Octopus*

*vulgaris* which showed a higher stress on the oral face of the rostrum (Fig. 6A). Under dragging force, rostra with a smaller sharpness index tend to have higher stress on a large area of both oral and aboral rostrum faces (Fig. 6B).

For both compression and dragging models, stress was higher for longer and sharper rostra. This is in line with the stiffness results indicating that longer and sharper rostra might be more vulnerable to failure under a give force. No high stress pattern was seen in the *Grimptoteuthis sp.* rostrum, showing excellent compression and dragging load bearing abilities. Rostra of *Sepia officinalis*, *Opisthoteuthis grimaldii* and *Rossia macrosoma* that are effective in bearing compression loads seem to be less effective in withstanding dragging force.

### Discussion

The size and rostrum shape variation present among cephalopod upper beaks impacts puncture ability and stress patterns during biting and dragging. Here, we quantified how key aspects of rostrum morphology—length, sharpness index, tip angle—affect the ability to puncture a target tissue and withstand stresses produced under loading conditions of simulating biting and dragging.

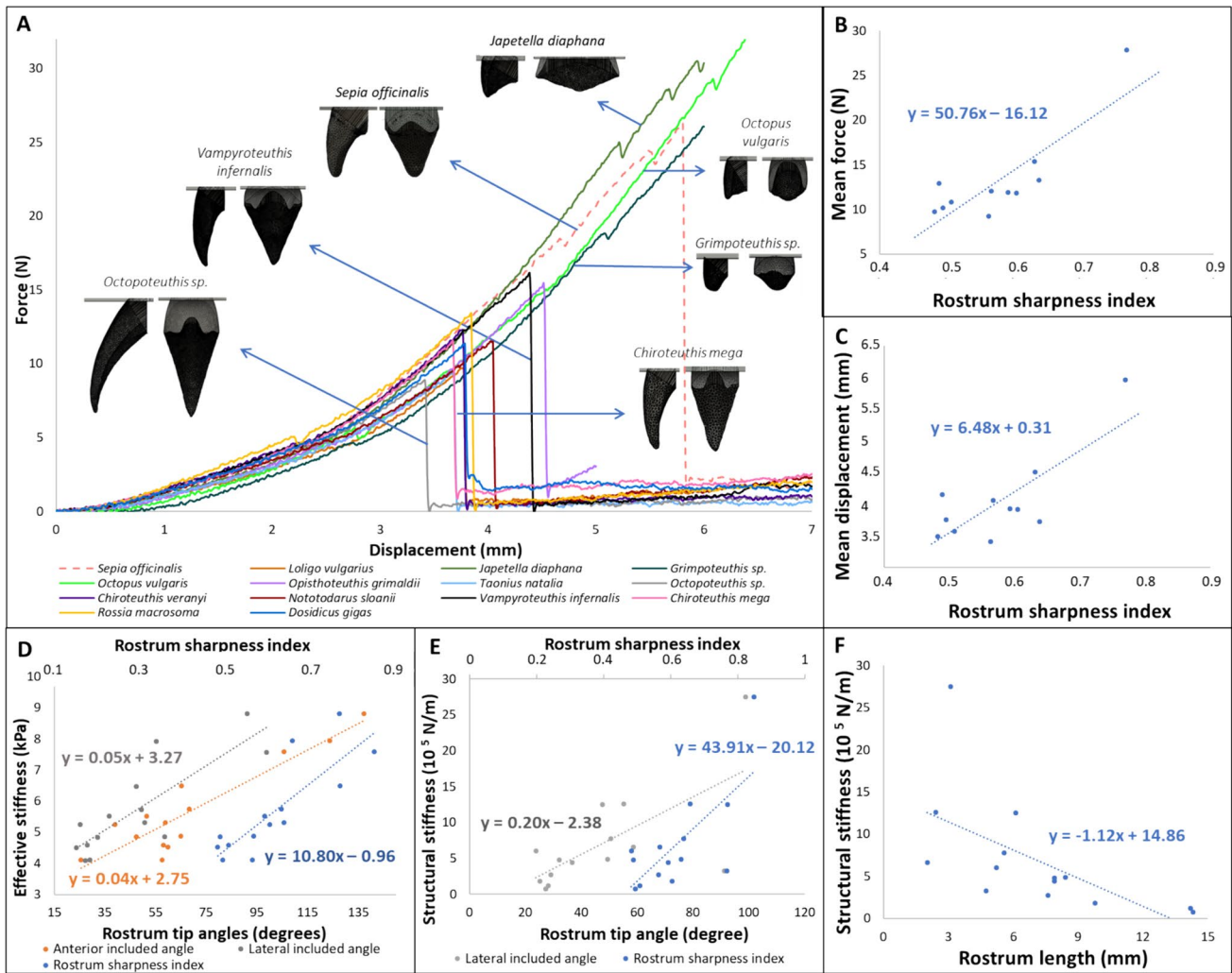


**Fig. 5** Morphology-driven puncture test and FEA results. **A** Force–displacement graph of the first set of the morphology-driven puncture tests. **B–F** Linear regression between **B** the penetration force and the cephalopod upper beak rostrum sharpness index; **C** the penetration displacement and the cephalopod upper beak rostrum sharpness index; **D** the linear region slope of the force–displacement graphs and

the cephalopod upper beak rostrum included angles and the sharpness index; **E** the cephalopod rostrum structural stiffness (obtained from the FEA compression test), the upper beak rostrum lateral included angle and the sharpness index; **F** the cephalopod rostrum structural stiffness (obtained from the FEA compression test) and the length of the rostrum models used in the FEA simulation

### The sharper the better?

Here, we observed that the rostrum sharpness, quantified by the sharpness index, is the primary morphological trait correlated with puncture performance. The sharper the rostrum tip, the less force required to puncture a given target, the opposite being true for blunt rostra. In our experiments, the rostra of octopodiforms (*Octopus vulgaris*, *Grimpoteuthis sp.*, and *Japetella diaphana*) failed to puncture the target with the maximum force used in this study. Therefore, once the global effect of size is removed, these species perhaps require a higher bite force than others to puncture a given tissue or alternatively do not puncture but rather fracture prey. We note that *Opistoteuthis grimaldi* did succeed in

puncturing the target with a rostrum shape and tip angle similar to *Grimpoteuthis sp.* However, *O. grimaldi* has a sharper rostral tip, explaining its greater puncture ability. The fact that the sharpness index (the radius of curvature of the tip extremity) seems more impactful than tip angles (included angle of the rostrum extremity) shows that the size of the contact point between the rostrum and prey is the determining factor in puncture efficiency (Anderson 2018). Therefore, wear on the rostrum tip related to age and use would perhaps result in a decrease in puncture performance. The beak of cephalopods is composed of a mix of chitin and cross-linked proteins (Tan et al. 2015), and exhibits a gradient of biomechanical properties from a stiff rostrum to more flexible posterior parts (Miserez et al. 2008, 2010).



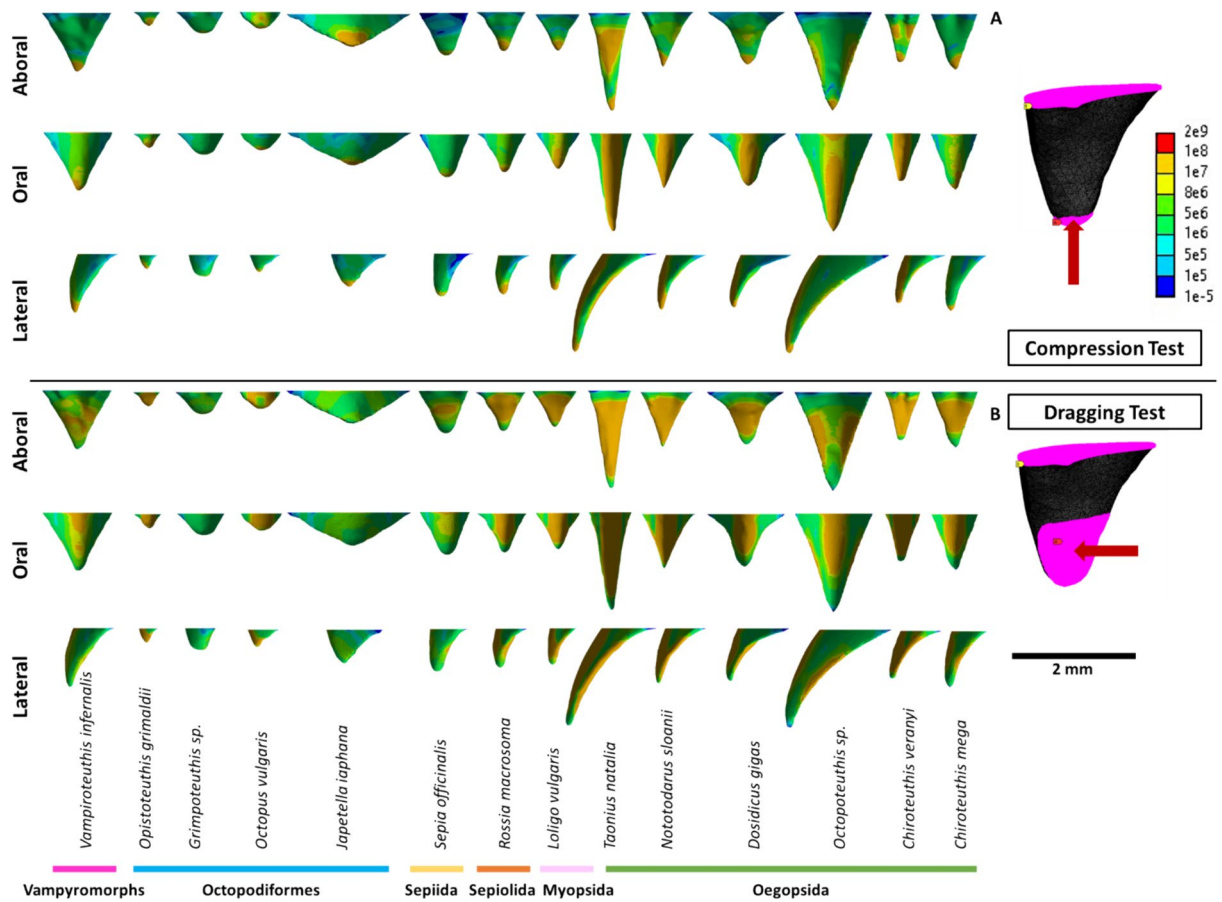


**Fig. 6** Von Mises stress pattern from FEA compression and dragging test on the upper beak rostra of 14 species. **A** Von Mises stress contour plots of the compression test with an indication of the constraints and loads. **B** Von Mises stress pattern plots for the dragging test. For both, the constraints and loads are illustrated on the rostra on

the right (pink, red arrow represent the load direction). Stress pattern colour legend is in Pa. Colour bars represent the cephalopod families using the colour code present on the phylogeny in Fig. 1

**Table 2** The statistical analysis results of the FEA compression tests (Bold numbers: p-value < 0.05)

Test parameter	Beak characteristic	Linear regression coefficient	Standard error	R square	F	P-value (significant F)
Structural stiffness	Rostrum scaling factor	2.30	0.03	0.999	4748.06	<b>&lt; 0.001</b>
	Rostrum length	-1.12	0.42	0.37	7.19	<b>0.020</b>
	Rostrum base area	-0.21	0.14	0.15	2.11	0.172
	Rostrum volume	-0.05	0.03	0.16	2.27	0.158
	Anterior included angle	0.11	0.06	0.25	3.90	0.072
	Lateral included angle	0.20	0.06	0.45	9.98	<b>0.008</b>
	Sharpness index	43.91	12.25	0.52	12.85	<b>0.004</b>
Penetration force	Structural stiffness	1.22	0.30	0.64	16.26	<b>0.003</b>
Penetration displacement	Structural stiffness	0.15	0.05	0.54	10.69	<b>0.010</b>
Slope of the linear region	Structural stiffness	2.57	1.14	0.30	5.02	<b>0.045</b>

In the common cuttlefish *Sepia officinalis*, rostrum stiffness also increases during ontogeny (Souquet et al. 2023). Therefore, cephalopod beaks may be locally reinforced to limit the effects of wear over time, preserving the sharpness of their rostra and thus maintaining an effective puncturing bite through life.

In vertebrates, it has been shown that sharper teeth induce less cracking but rather create an indentation during biting. On the other hand, blunter teeth are more likely to produce fractures in the food item rather than perforating it (Lucas 2004). Thus, the blunt rostra observed in octopodiforms are not optimized for puncturing but rather for creating cracks in prey to break it into pieces. This could be achieved either through the application of a strong bite force over a larger area covered by the rostrum or through a three-point bending action, with one point on the upper beak rostrum tip, and the two others on the lower beak rostrum edges (Fig. 1). This biting pattern aligns with the known feeding habits of benthic octopodiforms displaying short and blunt rostra that consume stiff and brittle prey such as crustaceans or shells. In captivity, octopuses consume only the soft parts of their prey, the hard parts being discarded at the bottom of the tank (Altman and Nixon 1970). Therefore, octopodiforms seems to have develop strategies to consume hard prey by fracturing the hard parts with their beaks, exposing the soft flesh that can then be accessed by the radula.

### On the advantage of being small

Smaller rostra showed better abilities to puncture the target with lower forces and lower displacements compared to larger ones. The size variation in the rostrum results in a scaling of the tip. Smaller rostrum tips are able to transmit a given force on a smaller area of the prey, producing a higher pressure (force per unit area) resulting in a more effective puncture (Johnson 1985; Schofield et al. 2016). As a result, for a given shape, larger beaks are blunter than smaller ones. Beak size being correlated to body mass (Xavier et al. 2023), larger animals with larger beaks will thus require sharper rostra to puncture a given prey, or a considerably higher bite force. This parameter, amongst others, may limit the maximum beak size in large species. Buccal mass shows a negative allometry against body mass in studied species (Morton and Nixon 1987; Nixon 1985; Kear 1994), and the largest species are known to have a relatively small beak compared to their body size. For example, the lower beak of a 500 kg *Architeuthis* only has a 30mm long rostrum (Clarke 1962). Hence, limiting maximal rostrum size might be an effective way to maintain an effective puncture without the high energetic cost of producing a large bite force.

The puncture advantage of smaller rostra may also impact feeding performance during ontogeny. A number of juveniles, including those of *Sepia officinalis*, are able to

bite relatively hard prey (Cherrel and Hubson 2005), while having no bite force performance compensation compared to adults that feed mainly on fish (Souquet et al. 2023). In this case, the small size of juveniles is already an advantage for puncturing prey compared to adults, and it is likely that this gain in performance is enough to obviate any compensation in terms of bite force to allow successful feeding.

### Why the long rostra?

Within the decapods, especially among Oegopsida, rostra of upper beaks tend not only to be sharp but also elongated, resulting in a slender claw-like shape. The length of the rostrum alone does not impact the puncture performance but is, however, negatively correlated with the structural stiffness calculated from FEA, indicating that long rostra are perhaps more prone to failure. Cephalopods use their arms to immobilize prey while biting with the beak, decreasing prey motion, and reducing lateral stress on the long rostra, reducing the risks of beak fracture due to struggling prey. Yet, the risks of rostrum fracture during biting remains high. In this context, what would be the selective advantage of having an elongated rostrum? Rostra are not cylindrical but frequently have a sub-triangular cross-section, with the aboral face being more or less rounded and sometimes possessing a groove on the oral face. The first hypothesis is that this morphology creates sharp lateral edges that would be able to achieve a shearing motion against the edges of the lower beak. Hence, a longer rostrum could allow for a larger shearing surface, enabling the cutting of relatively soft and elastic prey that a puncture type of bite would otherwise only indent. This is consistent with observations of wear patterns on cuttlefish beaks at various growth stages, showing a highly worn jaw angle on both upper and lower beaks, suggesting stress related to feeding in this area (Souquet et al. 2023). A second hypothesis is that longer rostra have a longer out-lever arm, which reduces the force transferred to the bite point but increases the beak closing speed. As most biological tissues are viscoelastic, their response to a given stress is dependent on its rate of application (Burstein and Frankel 1968; Kunzek et al. 1999; Vogel 2013; Anderson 2018). With an increase in strain rate, materials become stiffer, more resistant to deformation, allowing an easier creation of punctures in more elastic prey. Finally, elongation can also produce a more hydrodynamic shape, which could decrease energy loss to drag during underwater biting, thus allowing a faster bite with less force (Anderson 2018). All of these hypotheses would give an advantage to long rostrum bearers in biting and consuming soft and more elastic prey, such as fish. This is consistent with the fact that long rostra are mostly found in pelagic decapods, which predominantly feed on fish. Long rostra seem to be more versatile allowing

not only an initial puncture using the rostrum tip, but a cutting or shearing motion as well (Souquet et al. 2023).

### Prey toughness as a strong selective pressure

The highest puncture efficiency is reached by rostra having the smallest contact point with the prey item: a small rostrum point is better at concentrating bite force. An increase in puncture efficiency can therefore be achieved in two different ways: (1) increasing the rostrum tip sharpness, or (2) reducing the total size of the rostrum to obtain an overall smaller tip. However, both strategies are associated with structural weaknesses. Small rostra are less able to dissipate stress, while sharp rostra are less robust and more prone to failure which is aggravated by the fact that they are often elongated. Therefore, an evolutionary trade between size and sharpness for a given prey and bite force appears to exist. In vertebrates, the mechanical properties of food were hypothesized to provide a strong selective pressure for tooth morphology (Lucas 2004). Sharper teeth will create an indent in a prey while blunt teeth will have more difficulty to puncture the same prey but will more easily induce cracks and fractures depending on the material properties of that prey. In mammalian carnivores, prey material properties were also suggested to be related to teeth robusticity and therefore to their ability to tolerate stress (Pollock et al. 2022). Robust canines experiencing lower stress are found in carnivores regularly encountering hard foods while slender canines experiencing higher stresses are associated with carnivores biting into muscle and flesh. Unlike other animals bearing beaks, like birds or turtles, cephalopods use their sharp beaks (especially the upper one) to crush, pierce, and cut their prey, with an occlusion pattern that is different from that in birds and turtles (the aboral side of the upper beak is in occlusion with the oral side of the lower one, Fig. 1). Unexpectedly, the rostrum morphology is surprisingly similar to the canine crown outer shape (Pollock et al. 2022). Therefore, in terms of function, cephalopod upper beak rostra are more similar to teeth than to other animal's beaks. The pattern described above for vertebrate teeth is similar to the one observed in this study. Robust blunt rostra have an advantage for crack creation and fracture suitable for consumption of hard prey and are encountered in benthic octopods consuming a large proportion of crustaceans and shellfish. Slender sharp rostra will have an advantage for puncture and potentially shearing and cutting, suitable for consumption of softer and more elastic prey, and are encountered in pelagic decapods consuming a large proportion of fish. As a result, the hypothesis that the mechanical properties of the prey act as a strong selective

pressure on tooth morphology can be transferred to the upper beak rostrum of cephalopods.

### Conclusion

The rostrum sharpness is a crucial factor influencing puncture performance. Sharper rostra as commonly observed in decapods require less force to puncture a target, whereas blunt rostra, as observed in octopods, require higher forces to puncture the same prey. Therefore, with age, increase in beak size and wear of the rostrum tip may lead to a decline in puncture performance. Smaller rostra have a natural puncture advantage as their tips transmit a given force over a smaller area compared to larger ones, generating higher pressure and more effective punctures. This may lead to limitation of the beak size in larger species to optimise puncture efficiency. The elongation of rostra, observed in pelagic decapods, raises questions about the selective advantages of such morphology. While longer rostra do not directly impact puncture performance, they are negatively correlated with structural stiffness, possibly increasing the risk of failure. Yet, this elongation could permit a shearing motion of the rostrum edges to cut soft, more elastic prey such as fish. Overall, the study highlights the intricate trade-offs between rostrum size, sharpness, and structural integrity, emphasizing the role of prey toughness as a selective pressure shaping cephalopod upper beak morphology.

**Supplementary Information** The online version contains supplementary material available at <https://doi.org/10.1007/s00227-024-04451-0>.

**Acknowledgements** This work was supported by a Human Frontier Science Program Long-Term fellowship awarded to LS (LT000476/2021-L). We warmly thank the Bmade facility for the 3D printing and Juan Leal for his invaluable help conducting the puncture experiments.

**Author contributions** SM, SE, IR, AH, MM and LS contributed to the study conception and design. Material preparation, data collection and analysis were performed by SW, with contributions from MR, MD and LS. The first draft of the manuscript was written by SW and LS and all authors commented on previous versions of the manuscript. All authors read and approved the final manuscript.

**Funding** This work was supported by a Human Frontier Science Program Long-Term fellowship (LT000476/2021-L) awarded to LS.

**Data availability** The material and datasets generated and analysed during the current study are available from the corresponding author on reasonable request.

### Declarations

**Conflicts of interest** The authors have no relevant financial or non-financial interests to disclose.

**Open Access** This article is licensed under a Creative Commons Attribution 4.0 International License, which permits use, sharing, adaptation, distribution and reproduction in any medium or format, as long as you give appropriate credit to the original author(s) and the source, provide a link to the Creative Commons licence, and indicate if changes were made. The images or other third party material in this article are included in the article's Creative Commons licence, unless indicated otherwise in a credit line to the material. If material is not included in the article's Creative Commons licence and your intended use is not permitted by statutory regulation or exceeds the permitted use, you will need to obtain permission directly from the copyright holder. To view a copy of this licence, visit <http://creativecommons.org/licenses/by/4.0/>.

## References


- Altman JS, Nixon M (1970) Use of the beaks and radula by *Octopus vulgaris* in feeding. *J Zool* 161(1):25–38. <https://doi.org/10.1111/j.1469-7998.1970.tb02167.x>
- Anderson PS (2018) Making a point: shared mechanics underlying the diversity of biological puncture. *J Exp Biol* 221(22):jeb187294. <https://doi.org/10.1242/jeb.187294>
- Bidder AM, Wilbur KM, Yonge CM (1966) Feeding and digestion in cephalopods. *Physiology of Mollusca* 2:97–124
- Burstein AH, Frankel VH (1968) The viscoelastic properties of some biological materials. *Ann N Y Acad Sci* 146(1):158–165. <https://doi.org/10.1111/j.1749-6632.1968.tb20280.x>
- Cherel Y, Hobson KA (2005) Stable isotopes, beaks and predators: a new tool to study the trophic ecology of cephalopods, including giant and colossal squids. *Proc R Soc B: Biol Sci* 272(1572):1601–1607. <https://doi.org/10.1098/rspb.2005.3115>
- Clarke MR (1962) The identification of cephalopod "beaks" and the relationship between beak size and total body weight. *Bulletin of the British Museum (Natural History). Zoology* 8:419–480
- Clarke MR (1986) A handbook for the identification of cephalopod beaks. Clarendon Press, Oxford University
- Freeman PW, Weins WN (1997) Puncturing ability of bat canine teeth: the tip. In: Yates TL, Gannon WL, Wilson DE (eds) *Life Among the Muses Papers in Honor of JS Findley*. Albuquerque, NM, Special Publication 3, Museum of Southwestern Biology, pp 151–157
- Ibáñez CM, Riera R, Leite T, Díaz-Santana-Iturrios M, Rosa R, Pardo-Gandarillas MC (2021) Stomach content analysis in cephalopods: past research, current challenges, and future directions. *Rev Fish Biol Fisheries* 31:505–522. <https://doi.org/10.1007/s11160-021-09653-z>
- Jereb P, Roper CF, Norman MD, Finn JK (2014) *Cephalopods of the world: an annotated and illustrated catalogue of cephalopod species known to date, vol 3*. Food et Agriculture Organization of the United Nations, Rome
- Jereb P, Roper CFE (eds) (2005) *Cephalopods of the world: an annotated and illustrated catalogue of cephalopod species known to date, vol 4*. Food et Agriculture Organization of the United Nations, Rome
- Jereb P, Roper CFE (eds) (2010) *Cephalopods of the world: an annotated and illustrated catalogue of cephalopod species known to date, vol 4*. Food et Agriculture Organization of the United Nations, Rome
- Johnson KL (1985) *Contact Mechanics*. Cambridge University Press
- Kear AJ (1994) Morphology and function of the mandibular muscles in some coleoid cephalopods. *J Mar Biol Assoc UK* 74(4):801–822
- Kunzck H, Kabbert R, Gloyna D (1999) Aspects of material science in food processing: changes in plant cell walls of fruits and vegetables. *Zeitschrift Für Lebensmitteluntersuchung Und-Forschung A* 208:233–250
- Lucas PW (2004) *Dental functional morphology: how teeth work*. Cambridge University Press
- Messenger JB, Young JZ (1999) The radular apparatus of cephalopods. *Phil Trans R Soc Lond B: Biol Sci* 354(1380):161–182. <https://doi.org/10.1098/rstb.1999.0369>
- Miserez A, Schneberk T, Sun C, Zok FW, Waite JH (2008) The transition from stiff to compliant materials in squid beaks. *Science* 319(5871):1816–1819. <https://doi.org/10.1126/science.1154117>
- Miserez A, Rubin D, Waite JH (2010) Cross-linking chemistry of squid beak. *J Biol Chem* 285(49):38115–38124. <https://doi.org/10.1074/jbc.M110.161174>
- Morton N, Nixon M (1987) Size and function of ammonite aptychi in comparison with buccal masses of modern cephalopods. *Lethaia* 20(3):231–238. <https://doi.org/10.1111/j.1502-3931.1987.tb02043.x>
- Nixon M (1985) Capture of prey, diet and feeding of *Sepia officinalis* and *Octopus vulgaris* (Mollusca: Cephalopoda) from hatchling to adult. *Vie Et Milieu/Life & Environment* 35:255–261
- Nixon M (1987) *Cephalopod diets. Cephalopod Life cycles 2*. Academic Press, London, pp 201–219 (ISBN 012130023)
- Pollock TI, Panagiotopoulou O, Hocking DP, Evans AR (2022) Taking a stab at modelling canine tooth biomechanics in mammalian carnivores with beam theory and finite-element analysis. *R Soc Open Sci* 9(10):220701. <https://doi.org/10.1098/rsos.220701>
- Rodhouse PG, Nigmatullin CM (1996) Role as consumers. *Phil Trans R Soc Lond B: Biol Sci* 351(1343):1003–1022. <https://doi.org/10.1098/rstb.1996.0090>
- Roscian M, Herrel A, Zaharias P, Cornette R, Fernandez V, Kruta I, Cherel Y, Rouget I (2022) Every hooked beak is maintained by a prey: ecological signal in cephalopod beak shape. *Funct Ecol* 36:2015–2028. <https://doi.org/10.1111/1365-2435.14098>
- Roscian M, Souquet L, Herrel A, Uyeno T, Adriaens D, De Kegel B, Rouget I (2023) Comparative anatomy and functional implications of variation in the buccal mass in coleoid cephalopods. *J Morphol* 284(6):e21595. <https://doi.org/10.1002/jmor.21595>
- Schofield RMS, Choi S, Coon JJ, Goggans MS, Kreisman TF, Silver DM, Nesson MH (2016) Is fracture a bigger problem for smaller animals? force and fracture scaling for a simple model of cutting, puncture and crushing. *Interface Focus* 6:20160002. <https://doi.org/10.1098/rsfs.2016.0002>
- Souquet L, Basuyaux O, Guichard G, Herrel A, Rouget I, Evans S, Moazen M (2023) The growth of the buccal mass in *Sepia officinalis*: functional changes throughout ontogeny. *Mar Biol* 170(7):82. <https://doi.org/10.1007/s00227-023-04224-1>
- Tan Y, Hoon S, Guerette PA, Wei W, Ghadban A, Hao C, Miserez A, Waite JH (2015) Infiltration of chitin by protein coacervates defines the squid beak mechanical gradient. *Nat Chem Biol* 11(7):488–495. <https://doi.org/10.1038/nchembio.1833>
- Uyeno TA, Kier WM (2005) Functional morphology of the cephalopod buccal mass: a novel joint type. *J Morphol* 264(2):211–222. <https://doi.org/10.1002/jmor.10330>
- Uyeno TA, Kier WM (2007) Electromyography of the buccal musculature of octopus (*Octopus bimaculoides*): a test of the function of the muscle articulation in support and movement. *J Exp Biol* 210(1):118–128. <https://doi.org/10.1242/jeb.02600>
- Van De Berg NJ, De Jong TL, Van Gerwen DJ, Dankelman J, Van Den Dobbelen JJ (2017) The influence of tip shape on bending force during needle insertion. *Sci Rep* 7(1):40477. <https://doi.org/10.1038/srep40477>
- Villanueva R, Perricone V, Fiorito G (2017) Cephalopods as predators: a short journey among behavioral flexibilities, adaptations, and feeding habits. *Front Physiol* 8:598. <https://doi.org/10.3389/fphys.2017.00598>
- Vogel S (2013) *Comparative biomechanics: life's physical world*. Princeton University Press

- Xavier J, Chérel Y (2021) Cephalopod beak guide for the Southern Ocean: An update on taxonomy (revised edition). British Antarctic Survey, Cambridge, p 129
- Xavier JC, Golikov AV, Queirós JP, Perales-Raya C, Rosas-Luis R, Abreu J, Bello G, Bustamante P, Capaz JC, Dimkovikj VH, González ÁF, Guímaro H, Guerra-Marrero A, Gomes-Pereira JN, Hernández-Urcera J, Kubodera T, Laptikhovskiy V, Lefkadiou E, Lishchenko F, Luna A, Liu B, Pierce GJ, Pissarra V, Reveillac E, Romanov EV, Rosa R, Roscian M, Rose-Mann L, Rouget I, Sánchez P, Sánchez-Márquez A, Seixas S, Souquet L, Varela J, Vidal EAG, Chérel Y (2023) The significance of cephalopod

beaks as a research tool: an update. *Front Physiol* 14:1140110. <https://doi.org/10.3389/fphys.2022.1038064>

**Publisher's Note** Springer Nature remains neutral with regard to jurisdictional claims in published maps and institutional affiliations.

## Authors and Affiliations

Simeng Wang<sup>1</sup> · Marius Didziokas<sup>1</sup> · Marjorie Roscian<sup>2</sup> · Susan Evans<sup>3</sup> · Isabelle Rouget<sup>4</sup> · Anthony Herrel<sup>5,6,7,8</sup> · Mehran Moazen<sup>1</sup> · Louise Souquet<sup>1</sup> 

✉ Louise Souquet  
l.souquet@ucl.ac.uk

<sup>1</sup> Department of Mechanical Engineering, University College London, London, UK

<sup>2</sup> IVM Technologies SAS, Marseille, France

<sup>3</sup> Centre for Integrative Anatomy, Department of Cell and Developmental Biology, University College London, London, UK

<sup>4</sup> Centre de Recherche en Paléontologie-Paris (CR2P), UMR 7207, Muséum National d'Histoire Naturelle, SU, CNRS, Paris, France

<sup>5</sup> Département AVIV, UMR CNRS 7179 MECADEV, CNRS/MNHN, Paris, France

<sup>6</sup> Department of Biology, Evolutionary Morphology of Vertebrates, Ghent University, Ghent, Belgium

<sup>7</sup> Department of Biology, University of Antwerp, Wilrijk, Belgium

<sup>8</sup> Naturhistorisches Museum Bern, Bern, Switzerland